

**ROTOR LOADS COMPUTATION USING SINGULARITY METHODS AND APPLICATION  
TO THE NOISE PRODUCTION**

J. Haertig, M. Schaffar, P. Gnemmi  
French German Research Institute (ISL)  
BP 34, 68301 SAINT LOUIS (France)

Abstract

The paper presents two methods used to compute the unsteady loads on a rotor in order to predict blade vortex interaction (BVI) noise. Both are based on the potential flow theory of incompressible inviscid fluid.

The first one is a 2D analysis using a conformal mapping and point vortices. The comparison with experimental results obtained in a water channel shows that the unsteady lift is in good agreement with the computed one. Thereafter a pseudo 3D emission is proposed.

The second one is a numerical 3D simulation of the unsteady flow around a rotor. A vortex lattice is used to model the thin blades of a rotor and their wakes which are built up step by step.

A local conformal mapping is used to thicken the blade in order to obtain the unsteady pressure coefficients  $C_p$ .

These coefficients are the input data of an acoustic code based on the Ffowcs-Williams and Hawkings equation which gives the loading noise and the thickness noise. Some tests have shown that the results are very sensitive to the mechanical parameters of the rotor (collective pitch, etc.). Nevertheless, comparison with experimental results found in the literature shows the efficiency of the 3D method.

1. Introduction

Helicopter rotor noise is very impulsive under two different flight conditions. The first one is the low speed with acoustic pulse radiation when the blades are passing near their wakes. This is the blade vortex interaction (B.V.I.) noise. The second one is the high speed flight when the flow becomes transonic around the advancing blade. We are interested here in the first case which occurs in descent or low speed military flight over urban areas near heliports or during military operations. The helicopter rotor wake is composed of the wake of each blade which rolls up to generate a strong helical vortex system. All blades are then moving in a very disturbed vortical flow giving an unsteady pressure field radiating impulsive noise at great distance.

Most theoretical approaches to the acoustic problem are based on the Ffowcs-Williams and Hawkings equation which exhibits three types of acoustic sources. As explained in the next paragraph, the thickness noise is due to the volume of fluid displaced by the blade, the loading noise is related with the forces exerted by the fluid on the blade and the third one (volumic quadruple sources) is neglected here since the advancing tip Mach number  $M_{AT}$  remains below 0.8.

The thickness noise can be calculated when the shape of the blade and the kinematics of the rotor are known but the loading noise computation requires the knowledge of the unsteady local loads over the blade. It is then necessary to solve the aerodynamic problem of the flow around a rotor and to find some models representing the blade vortex interaction phenomenon.

A simple model is presented in the second section of the paper. It is based on the computation of the velocity potential in a 2D incompressible inviscid unsteady flow using conformal mapping. It gives the flow field around a Joukowski airfoil with known incident vortices modelling the vortical wake. These vortices and the wake of the tested airfoil itself are modelled by point singularities. Analytic expressions are obtained so that aerodynamic coefficients (pressure, lift, moment, etc.) are computed very quickly. Experiments conducted in the water channel at ISL check the validity of this model so that a "2.5D" extension was developed to have a more realistic representation of a rotor BVI. The tip vortex is a helicoidal line vortex with the same shape as the blade tip trajectory. The blade is divided in span slices and for each span section the 2D method is used. The noise may then be computed and the results are compared with the experiments. This very simple model needs very little computation time but the rotor wake is only roughly modelled by a frozen line vortex the intensity and height of which, with respect to the blade, must first be known by other means.

To be freed from any empirical data, a 3D numerical simulation of the flow around a multibladed rotor was developed and is presented in the third section. It is based on the Prandtl lifting surface theory of a thin airfoil. It is a time step method using a vortex lattice to model the blades and their free wakes.

Copyright 1190 by the American Institute of Aeronautics and Astronautics Inc. and the International Council of the Aeronautical Sciences. All rights reserved.

This new method needs only the geometry of the blades, the kinematic parameters of the rotor and the flight conditions. A local 2D conformal transformation is used to obtain the pressure coefficients  $C_p$  on the thick blade, these coefficients being the input data of the acoustic code. Different tests are made to show the sensitivity of global rotor parameters (such as the thrust coefficient  $C_T$ ) to a little change in some rotor parameters.

Moreover, acoustic results obtained with the 3D method are presented and compared with the same experimental results as those previously indicated.

## II. Acoustic analysis

The acoustic analysis is based on the work of Lawson, Ffowcs-Williams, Hawkins and Farassat<sup>1,2,3</sup>. When a rigid body limited by the closed surface  $S$  moves at subsonic speed, the quadruple source term may be neglected and it can be shown that the far field acoustic pressure  $p$  radiated at an observer position  $\vec{x}$  is the sum of the thickness noise  $p_t$  and loading noise  $p_\ell$  given by:

$$p_t(\vec{x}, t) = \frac{-1}{4\pi} \int_S \left[ \frac{\rho_0}{|\vec{r}|(1-M_r)^2} \left( \frac{\partial v_n}{\partial \tau} + \frac{v_n}{1-M_r} \frac{\partial M_r}{\partial \tau} \right) \right] dS(\vec{y})$$

$$p_\ell(\vec{x}, t) = \frac{-1}{4\pi} \int_S \left[ \frac{1}{a|\vec{r}|(1-M_r)^2} \left( \frac{\partial \ell_r}{\partial \tau} + \frac{\ell_r}{1-M_r} \frac{\partial M_r}{\partial \tau} \right) \right] dS(\vec{y})$$

when:  $S$  is the surface of the moving blade

$\vec{y}$  is the position of the surface source element  $dS$

$\vec{v}$  is the velocity of that element

$\vec{v}_n = \vec{v} \cdot \vec{n}$   $\vec{n}$  being the exterior unit normal at  $dS$

$\vec{r} = \vec{x} - \vec{y}$

$$M_r = \frac{\vec{v} \cdot \vec{r}}{a|\vec{r}|}$$

$\tau$  = emission time corresponding to the observer time  $t$

$$\tau = t - \frac{|\vec{r}|}{a}$$

$a$  = sound speed of the medium at rest

$\vec{\ell}$  = force per unit of area exerted on  $S$  by the fluid

$$\ell_r = \vec{\ell} \cdot \frac{\vec{r}}{r}$$

If viscous stress is neglected,  $\ell_r \sim C_p \vec{n} \cdot \vec{r} / |r|$ . The above-mentioned integrals are calculated by dividing the blade surface  $S$  in small quadrilateral elements  $dS(\vec{y})$  where the values of  $\vec{v}_n$ ,  $\ell_r$ ,  $M_r$ , etc. are constant and equal to their value at the centroid of the elements. The acoustic code is similar to the code of Farassat<sup>4</sup> and runs in the time domain.

The case of a moving observer is generally chosen in order to simulate the experiments (a fixed rotor and fixed microphones are set in a wind tunnel).

At each observer time  $t$  and position  $\vec{x}(t)$  the blade surface  $S$  is scanned to know the position and the strength of each source element  $dS(\vec{y})$  at the corresponding emission time  $\tau(t, \vec{x}, \vec{y})$ . The acoustic pressure  $p(t)$  is the addition of each individual contribution.

The thickness noise  $p_t$  is readily calculated when the shape of the blades and the kinematics of the rotor are known.

On the other hand, the loading noise  $p_\ell$  (which is responsible for impulsive pressure when BVI occurs) may be calculated only if the surface blade pressure coefficients  $C_p(\vec{y}, \tau)$  are known.

It is then necessary to find an aerodynamic model of the blade vortex interaction phenomenon.

## III. 2D aerodynamic model and pseudo 3D extension

### 2D model

A simple approach is to consider the 2D problem. We look at the velocity field of an unsteady incompressible potential flow around a Joukowski airfoil in the presence of known incident vortices simulating the incoming vortical flow. The incident vortices and the wake of the airfoil are modelled by point singularities.

This analysis leads to analytic expressions for the complex potential, aerodynamic coefficients etc. used in a code named VOPRO which gives the pressure coefficients  $C_p$  and the lift coefficient  $C_z$  as a function of time<sup>5</sup>.

The input data are:

- the thickness and the angle of attack of the airfoil;
- the number of discrete incident vortices, their respective intensities and their initial locations.

At each time step the Joukowski condition and total circulation conservation law give the shed vorticity in the wake of the airfoil. This code runs very fast and a large amount of weak incident vortices may be used to simulate a viscous vortex. Results given by this code have been compared with those given by the more sophisticated 3D code (based on the method presented in the next section). The evolution of the lift coefficient  $C_z$  versus the incident vortex horizontal position is shown on figure 1.

Moreover, numerical results have been compared with experimental ones obtained in the water channel facility of ISL. A pitching airfoil acting as a vortex generator is followed downstream by the tested airfoil. The incident vorticity field is measured with a 2D Laser Doppler Anemometer. The lift

of the tested airfoil is measured with a force balance<sup>6</sup>. Figure 2 gives an example of the instantaneous vorticity field (its vorticity curves) and figure 3 shows the good agreement of calculated and measured lift coefficients in spite of the low experimental Reynolds number ( $20 \times 10^3$ ). The quantities shown are non dimensionalized with the upstream velocity  $v_\infty$  and airfoil chord  $c$ . Many tests have been made. They show that the thickness and the angle of attack have only a weak influence whereas the main parameters are the vortex intensity and height with respect to the leading edge of the airfoil.

This agreement leads to look for a more realistic simulation of a BVI based on this 2D analysis.

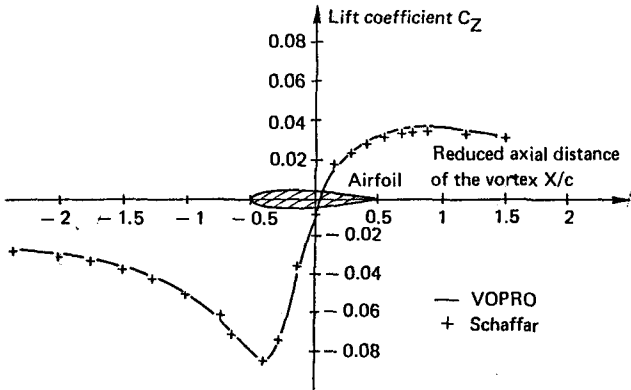


**Fig. 1 :** Airfoil lift coefficient as a function of vortex horizontal distance:  
initial vertical distance =  $-2c$   
vortex circulation =  $-0.5 U_\infty c$

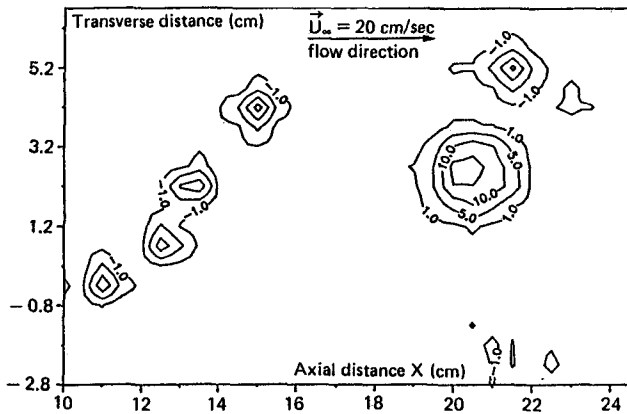


**Fig. 2 :** Vorticity field measurements:  
 $\alpha = 10$  deg,  $t = 940$  msec  
 $\Gamma_{max} = -0.52 U_\infty c$ ,  $\Gamma_{min} = +0.11 U_\infty c$ ,  
 $\omega_{max} = -17.2$ ,  $\omega_{min} = +17.6$

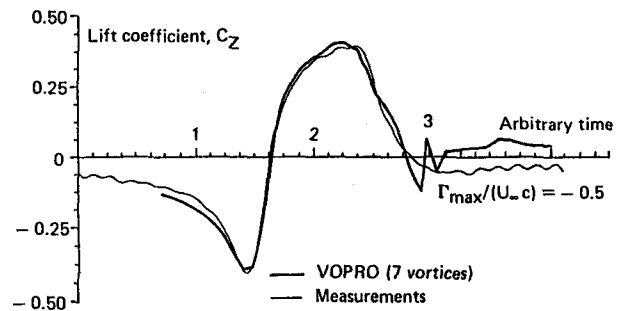


**Fig. 3 :** Comparison of measured and calculated lift coefficients for a vertical distance  $h/c = 0.13$

### Pseudo 3D extension

The blade tip vortex is sketched by the blade tip trajectory (epicycloidal line) with given intensity and height with respect to the rotating airfoil representing the advancing blade of a rotor (angular velocity  $\Omega$ , advancing speed  $V_a$ ).

We then consider the 2D problem in a plane perpendicular to the span at any span location (figure 4). Knowing at a given time the location of the vortex segment and the relative velocity of the blade section, we use VOPRO to compute the values of  $C_p$  on that blade cross section<sup>7</sup>. This "2.5D" extension has been applied to the AH1 OLS rotor which has often been used for acoustic investigations<sup>8</sup>. It is a two-bladed rotor with rectangular blades (thickness 9.7%, linear twist  $10^\circ$ ). Blade vortex interaction occurs at an advance ratio  $\mu = 0.164$  and at advancing tip Mach number  $M_{AT} = 0.773$ .

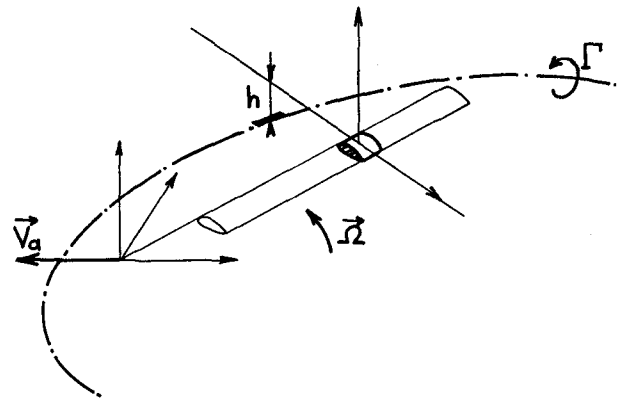


**Fig. 4 :** Heuristic 3D extension of the 2D model

The intensity of the line vortex is chosen equal to the circulation around the profile at half a chord from the tip deduced from the angle of attack at that span and the location is half a chord below the rotor disk. The computed  $C_p$  coefficients are fed as input data in the acoustic code to compute the pressure signature at locations corresponding

to microphone locations in the experiment. Figure 5 shows the measured and calculated pressure signals in various directions ( $\theta, \phi$ ) ( $\theta$  = horizontal angle,  $\theta = 0$  = forward direction,  $\phi$  = vertical angle,  $\phi < 0$  = under the rotor). These results look similar, then this method which is very fast may be convenient for parametric investigations. Nevertheless, it is necessary to know the location and intensity of the line vortex which is only a rough approximation of the unknown rotor wake. To get rid of any external parameters we develop a 3D computation of the flow around a rotor.

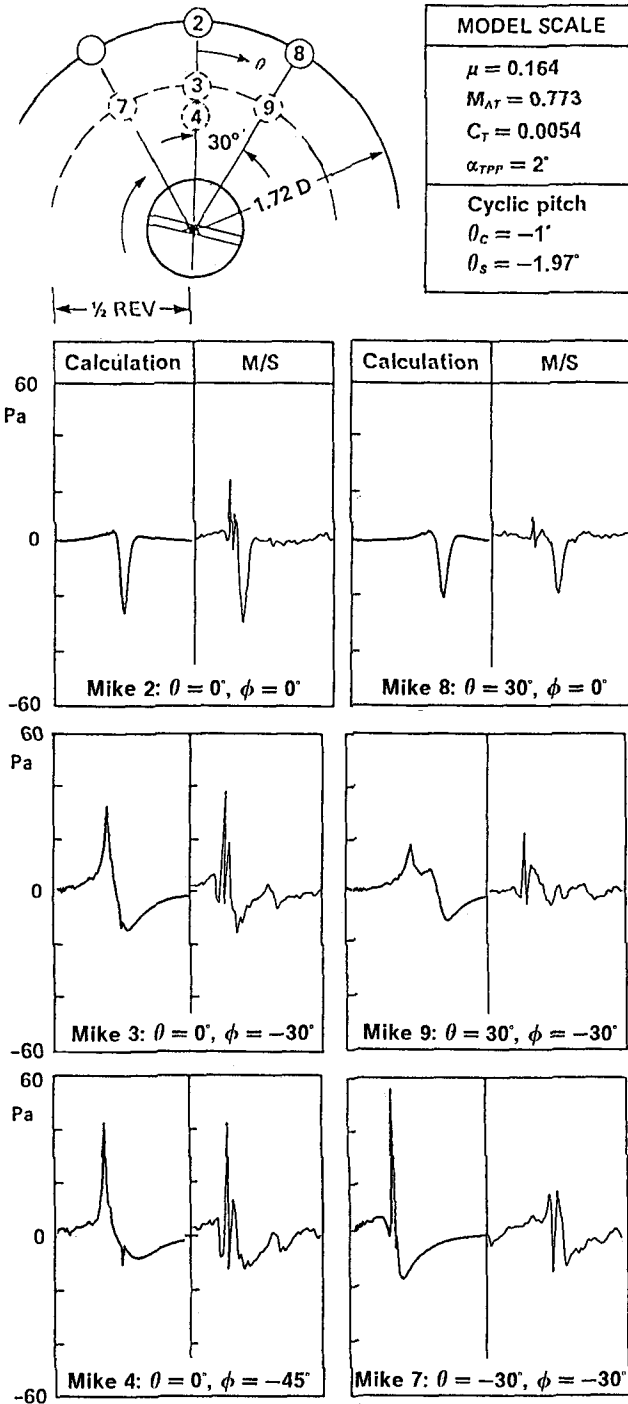


Fig. 5 : Measured and calculated acoustic pressure signals obtained with the extension of the 2D model

#### IV. 3D simulation of a rotor

The same assumptions as previously mentioned (incompressible inviscid potential flow) are made and the lifting surface theory is used. The blades are replaced by thin airfoils with the same plane form and twist. The thin airfoils are mapped with quadrilateral panels giving a spanwise and chordwise vortex lattice<sup>7</sup>. Each segment of the lattice supports a circulation which is determined at each time step. At  $t=0$  the blades begin to move according to the prescribed mechanical parameters of the rotor (angular velocity  $\Omega$ , pitch angle  $\theta$ , flapping angle  $\beta$  which depend on the azimuthal position  $\Psi$  of the blade) and a freestream velocity  $\bar{V}_\infty$  is set to simulate the advancing flight (climb, descent).

At each time step the circulation of the bound vortices is determined by the slip condition on the centroid of each panel and by writing that the total circulation arriving at each node of the lattice is zero. Moreover, a vortex segment is shed near the trailing edge to counterbalance the change of total circulation around the airfoil at each span section. The shed vortices are known and move freely under the action of all the other vortices and freestream velocity. The free wake of the blades is thus built up step by step as time goes on (figure 6).

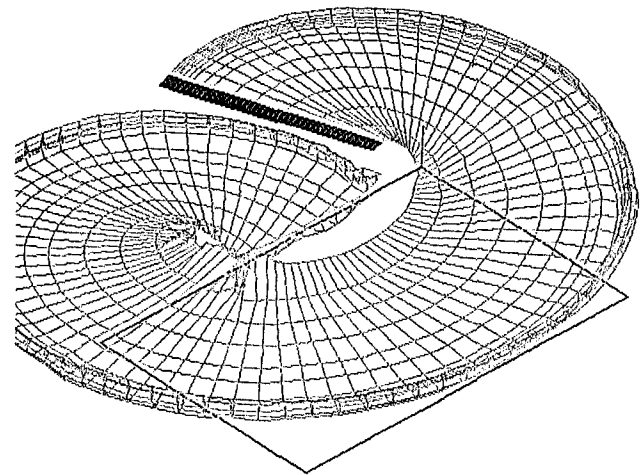


Fig. 6 : Blade and wake vortex lattice

Moreover, a local 2D conformal mapping is used in order to obtain the local pressure coefficient  $C_p$  of the thick blades. Assuming that the potential remains the same through the transformation, the "unsteady" Bernoulli equation gives the  $C_p$  and after an integration over the blades, the thrust coefficient

cient  $C_T$  is obtained<sup>10</sup>. As an example, figure 7 shows the evolution of  $C_T$  versus the azimuthal angle  $\Psi$  ( $\Psi = \Omega t$ ) for a hovering rotor. After the start up,  $C_T$  reaches a constant value very close to the experimental one (mean computed  $\bar{C}_T = 0.047$ , measured value  $C_T = 0.0045$ ). We have tested the sensitivity of this thrust coefficient to some rotor parameter variations. Figure 8 shows the case of a BO-105 rotor when the following parameters are slightly changed from their nominal values:

collective pitch ( $\theta_0$ ), longitudinal cyclic pitch ( $\theta_c$ ), longitudinal ( $\beta_c$ ) and transversal ( $\beta_s$ ) flapping angle, advance ratio ( $\mu$ ) and rotor shaft angle ( $\alpha_q$ ).

It is quite clear on this figure that every rotor parameter must be accurately known if we wish to check the calculation by comparison with experiments.

The 3D simulation was applied to the AH1-OLS rotor (see section 2) to compute the  $C_p$  and then the acoustic pressure signatures.

Theoretical results are presented on figure 9 together with the experimental ones previously shown. A fairly good agreement is generally found especially for noise radiation below the rotor disk ( $\phi < 0$ ) when BVI noise is important. In the rotor plane, however, some discrepancies appear but

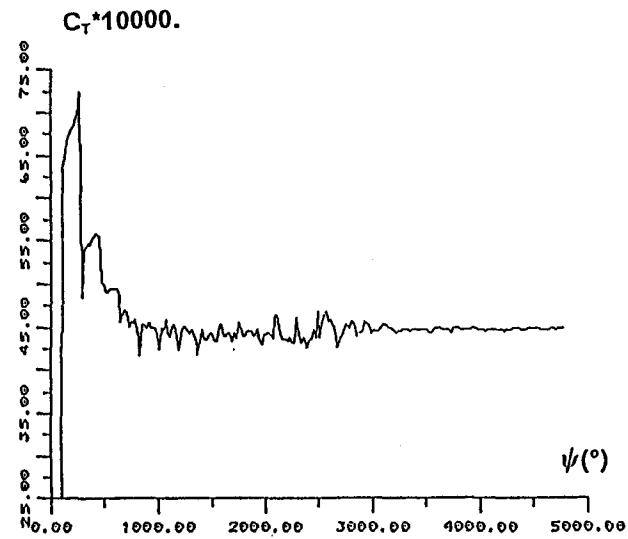


Fig. 7 : Evolution of the thrust coefficient for a hovering rotor (collect. pitch 10°, coning angle 3°)

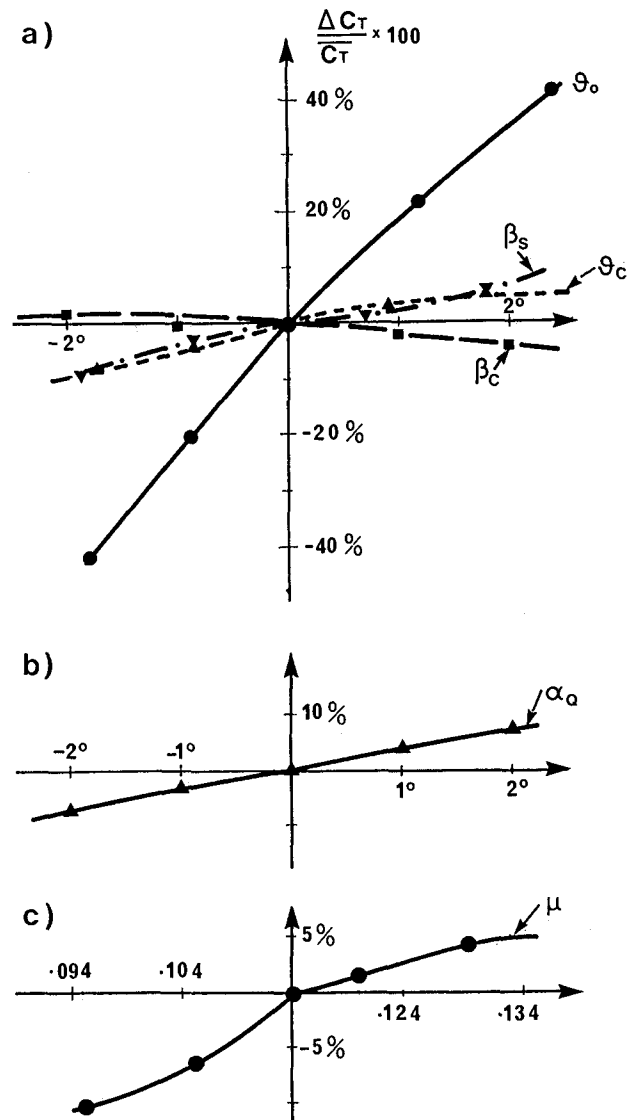


Fig. 8 : Low speed advancing flight (BO-105,  $\mu = 0.114$ )  
Thrust coefficient sensitivity to various parameters

- a) collective pitch ( $\theta_0$ ), longitudinal cyclic pitch ( $\theta_c$ ), flapping angle  $\beta_c$ ,  $\beta_s$
- b) rotor shaft angle with upstream velocity  $\alpha_q$
- c) advancing coefficient  $\mu$

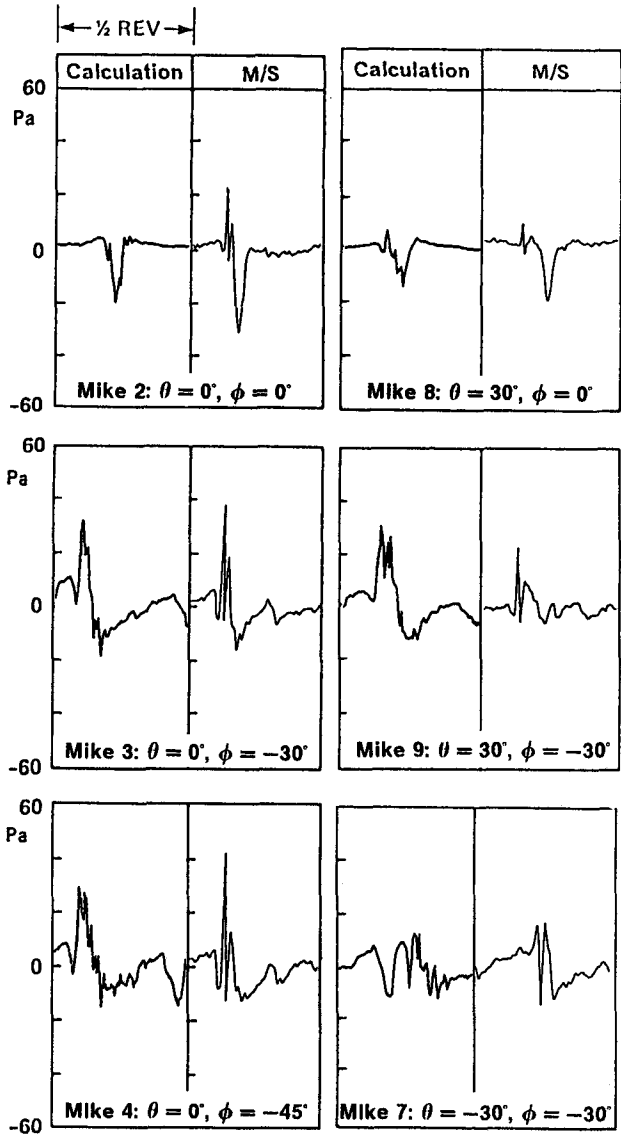
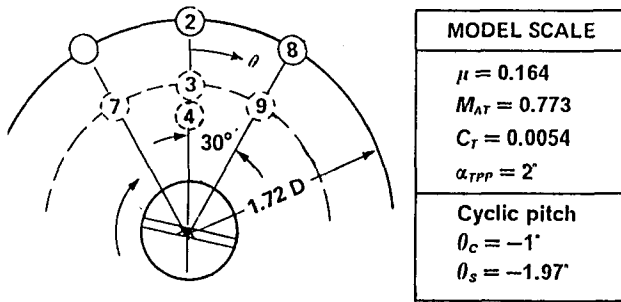


Fig. 9 : Measured and calculated acoustic pressure signals obtained with the 3D vortex lattice model

they may arise from uncertainty on some flight parameters. In fact it is found that the BVI noise (positive pulse) cancels the thickness noise (negative pulse) so that the peak to peak calculated pressure decreases. This kind of "destructive interference" may be sensitive to flight parameters (in that

particular case the cyclic flapping angles were unknown and taken equal to zero).

Figure 10 shows some calculated horizontal acoustic directivity curves when some parameters are changed. Like the thrust coefficient, the acoustic level results from an integration over the blade surfaces and it is then obvious that it depends heavily on the flight parameters, too.

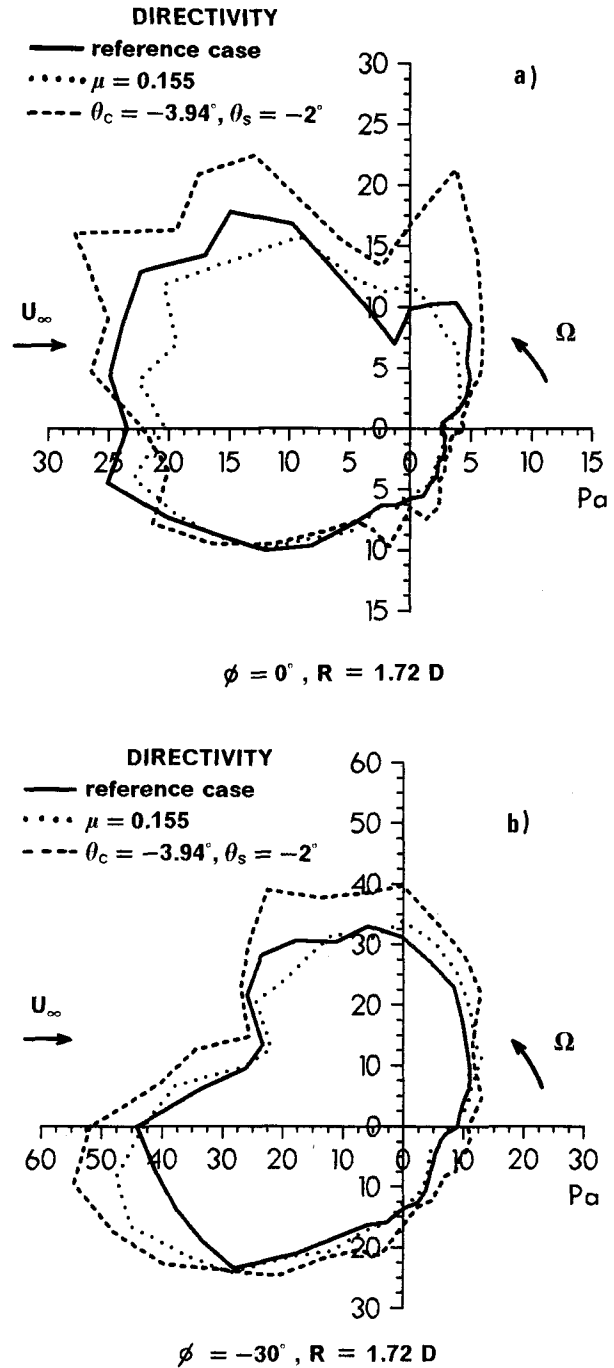


Fig. 10 : Horizontal directivity of noise radiated at a diameter of 1.72 from the center of the rotor a) in the rotor plane, b) 30° below the rotor plane

## V. Conclusions

The vortex lattice method seems to be useful to compute the flow around a helicopter rotor without any empirical data but at the price of computer time consumption.

The aerodynamical results may be used to predict the radiated blade vortex interaction noise.

The work is still in progress and some numerical and theoretical problems remain to be investigated keeping in mind the frame of the study (perfect potential flow). Nevertheless, we have shown that aerodynamic and aeroacoustic predictions agree with experimental results only if all the flight parameters are known and used as input data of the codes.

In the future, this method may be applied to the study of new "advanced blades", multicyclic pitch rotors, and to the coupling of aerodynamics with the kinematics of the rotor.

## Acknowledgment

This work has been conducted with the support of DRET. (Contracts 85-031, 88-214)

## References

- <sup>1</sup> Lawson M.V. "The sound field of singularities in motion", Proc. Royal Soc., A 286, p. 559 (1965)
- <sup>2</sup> Ffowcs Williams J.E., Hawkins D.L. "Sound generation by turbulence and surfaces in arbitrary motion", Phil. Trans. Royal Soc. of London, vol. 264, No. 1151, p. 321 (1969)
- <sup>3</sup> Farassat F. "Discontinuities in aerodynamics and aeroacoustics: the concept and applications of generalized derivatives", J.S.V. 55 (2), p. 165 (1977)
- <sup>4</sup> Farassat F., Succi G.P. "A review of propeller discrete frequency noise prediction technology with emphasis on two current methods for the time domain calculations", J.S.V. 71 (3), p. 399 (1980)
- <sup>5</sup> Haertig J., "Interaction entre un tourbillon et un profil d'aile (écoulement incompressible 2D)", "Wechselwirkung zwischen einem einfallenden Wirbel und einem Tragflügelprofil (inkompressible 2D-Strömung)", ISL report R 119/85 (1985)
- <sup>6</sup> Haertig J., Johé C., Schaffar M. "Interaction profil - tourbillon", "Profil/Wirbel-Wechselwirkung", ISL report R 125/87 (1987)
- <sup>7</sup> Gnemmi P., Haertig J., Johé C. "Modélisation d'interactions pale - tourbillon", "Modellierung von Rotorblatt/Wirbel-Wechselwirkungen", ISL report R 107/89 (1989)
- <sup>8</sup> Spletstoesser W.R., Schultz K.J., Boxwell D.A., Schmitz F.H., "Helicopter model rotor-blade vortex interaction impulsive noise: scalability and parametric variations", NASA Tech. Mem. TM-84A7
- <sup>9</sup> Konstadinopoulos P. "A vortex lattice method for general unsteady subsonic aerodynamics", M.S. Thesis, Dept. Eng. Virginia Polytechnic Inst. and State Univ. Blacksburg, Virginia (1981)
- <sup>10</sup> Schaffar M., Haertig J., Gnemmi P. "Aerodynamic loads and blade vortex interaction noise prediction", Fifth Europ. Rotorcraft Forum, paper No. 3, Sept. 1989, Amsterdam